Numerical and experimental study the effects of river width changes on flow characteristics in a flume

Numerical and experimental study the effects of river width changes on flow characteristics in a flume

S F Zhou[1], X K Wang[2], Q Y Yang[3] and Z W Huang[1]

[1]Jiangxi Institute of Water Sciences, Nanchang 330029, P.R. China

[2]State Laboratory of Hydraulic and Mountain River Engineering, Sichuan University, Chengdu, 610065, P.R. China.

[3]Hydraulics Research Department, Changjiang Scientific Research Institute, Wuhan 430010, P.R. China

corresponding author's e-mail address:512595913@qq.com

Abstract. The gradual characteristics of variations in transverse width often occur in mountain river because of the effect of geological conditions and river evolutions. This will influence flow and sediment transport due to the variations of flow structures resulted from the river width changes. A flume experiment that was conducted to explore how flow characteristics perform with the varied channel width, showing the connection of the flow parameters, flow rate and channel width. For example, the longitudinal water depth and velocity change along with the transition width of flume. On the other hand, a depth-averaged two-dimension model was proposed according to series of methods such as body-fitted coordinate, finite volume method, SIMPLER algorithm. The numerical results agreed well with the experimental observation in a flume, which showed that the model could reasonably simulate gradual channel transition flow. In addition, the validated numerical model was applied to simulate flow with different flow rates with the same imposed boundary condition in order to further analyse the effects of channel width variation on flow characteristics.

1. Introduction

In the realistic nature, various types of open-channels exist with respect to the different figures and shapes. In the fundamental works, straight open-channel is considered as the basic shape one have been extensively explored (Nezu and Nakagawa 1993; Afzalimehr and Anctil 2000; Wang et al. 2011), subsequently for reference in observation of other types of open-channel. For decades of study, the open-channel hydraulic literature has already been extended to bend flows and confluence flows, forming relative knowledge system in spite of some limitations and shortcomings (Blanckaert and Vriend 2005; Barbhuiya and Talukdar 2010; Weber et al 2001). However, open-channel with width variation is common in field. For example, the Jinma reach of Minjiang River ranges in width from about 300 to 1010 meters. The influence of Channel width variation is pronounced for sediment transport and river evolution. The gradual channel transition is typically characterized by non-uniform flow that also shows in bend, confluence or some other open-channels. When neglecting the channel width variation or when the channel width variation is tiny enough in terms of the mean channel width, the gradual channel transition can be considered as the straight open-channel. That is the point when studying the gradual channel transition.

Recently open-channel with width variation is drawing attention. Thomas M et al (1995) used a depth-averaged open-channel model to simulate flow in converging channel. Papanicolaou and Hilldale (2002) showed field work of a gradual expansion, describing the secondary currents, vertical profile distribution and turbulence. Nguyen T H et al (2007) studied the velocity and turbulence distributions of decelerating open-channel flow in gradual expansion. Based on numerical calculation, Armellini (2009) found that separated region of flow structures became obvious because of the bed form. Lucy (2010) found the change of river width was a critical factor in river evolution after extensive investigations. Singha (2011) observed that the turbulent kinetic energy would be adjusted along with channel planform. According to the study of experiment in a wide and narrow transformation channel, Paiement-Paradis (2011) discovered the change of velocity made a great contribution to the transportation of bed load. Yan X f (2011) focused on the local head loss of wide and narrow region in laboratory flume, the results indicated that the head loss coefficient in the diverging region was greater than any other region, that was to say the particular channel form had a great effects on the local head loss.

Although literatures above can show some aspects, the knowledge of hydraulics about open-channel with width variation is still relatively lacking. Thus more efforts should be put experimentally and numerically. In this paper, the effects of channel width variation on flow characteristics in a laboratory flume were studied both experimentally and numerically.

2. Experimental arrangement and program

Experiments were carried out in a flume which was 28m long, 0.5m deep, and width changes as a sine curve that was B=0.2sin(1.0472*x*+2.0944)+0.5 as shown in Figure 1. The widest section was 1.6m and the narrowest section was 0.6m. The flume was made of masonry with smooth painted walls by cement with the bed slope of 0.2%. There were 37 measured profiles as shown in Figure 2. A downward looking MicroADV was used to measure instantaneous velocity field. MicroADV has become a useful instrument in measuring 3D velocity field in laboratory and field environments by recording the Doppler shift produced by acoustic targets in the flow. The sampling volume of a MicroADV was located about 5 cm from the probe. The sampling frequency was set to 50HZ in this experiment. According to the width of each measured profiles, the velocity was measured at different transverse interval. Two experiments with different flow rates were conducted. One was Q=0.112m^3/s, the other was Q=0.1m^3/s.

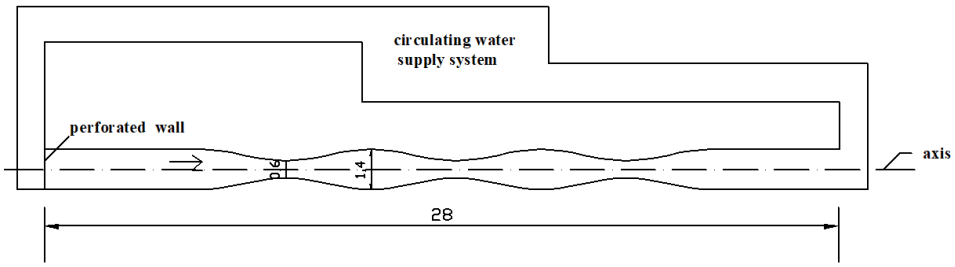

Figure 1. Scheme of self-circulation system of gradual channel, all numbers in [m].

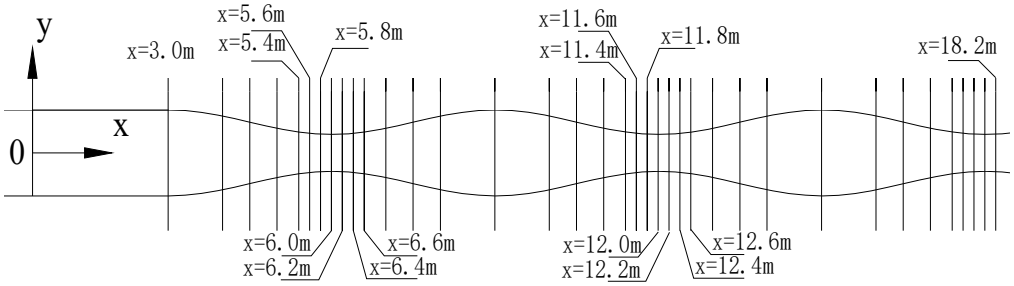

Figure 2. The distribution of measurement sections

3. Experimental results and analysis

3.1 Hydraulic conditions

Figure 3 to 4 show the hydraulic conditions in two flow rates. From Figure 3, we can see that water depth would change along with the gradual channel transition, the depth near the narrowest sections(x=6m, 12m, 18m)is lowest in central vertical plan, while highest near the widest sections(x=12m,15m). In Figure 4, the Froude number shows the opposite trend compared with the water depth. When 6m<x<6.4m, Fr>1, which means supercritical flow occurs. However, subcritical flow occurs in other sections where Fr<1. Thus we can conclude that channel with variation should influence flow pattern.

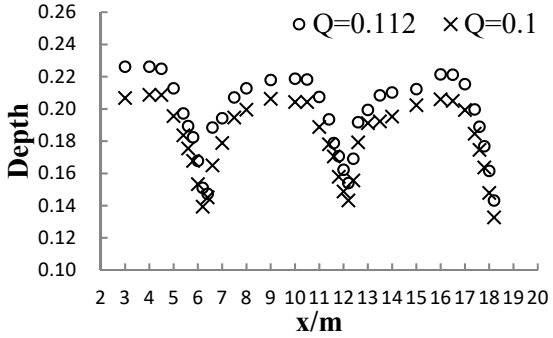

Figure 3. Average depth in central vertical plan

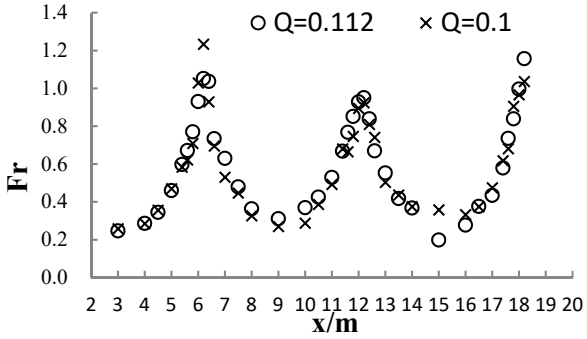

Figure 4. Froude number in central vertical plan

3.2 Velocity distributions

Velocity profile in central vertical plan of the flume is shown in Figure 5. The velocity curve is similar to the Froude number curve, which value decrease with increasing width of flume. In the narrowest section, the velocity reaches crest. In order to discuss velocity distribution, dimensionless design was used. Figure 6 shows the variation of u/u_* with Z/H where u is average velocity at measuring position z (distance from the channel bed), and u_* is shear velocity, H is water depth. From the figure we can see that there are zones (when 0.9<Z/H<1.0) where no data are available, because the sampling volume of MicroADV is valid about 5cm below the probe tip. In Figure 6, the data of cross-section with same width used same graphic symbol, but the hollow symbol represent data in diverging sections and the solid symbol in converging sections. Whether in diverging sections or converging sections, velocity decreased with increasing of channel width. In diverging sections, velocity first increase with increasing of depth then decreases at a height of about Z/H=0.5, but velocity increase with increasing depth all the time in converging sections, that could be attributed to the presence of hydraulic jump which is a transition from supercritical to subcritical flow (Figure 4).

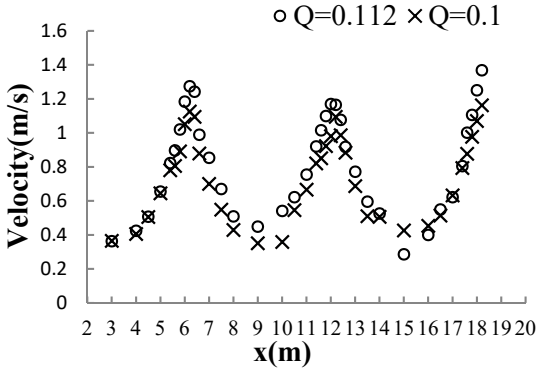

Figure 5. Averaged velocity profiles in central vertical plan

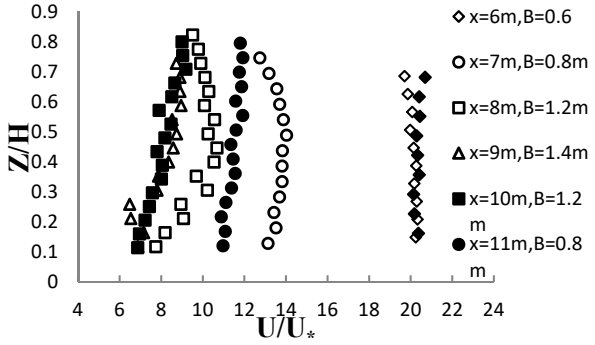

Figure 6. Averaged velocity profiles in mid-wide line of typical cross-sections(Q=0.112m^3/s)

3.3Turbulence intensity

Figure 7 shows that the distribution of turbulence intensity along the vertical line in typical sections. It can be seen that the turbulence intensity distribution in *x*-direction is similar to that in *y*-direction and both are stronger than that in *z*-direction. And the turbulence intensity increase with increasing of channel width. But in cross-sections with same width, the turbulence intensities in converging sections are stronger than that in diverging sections. Furthermore, at about $0<Z/H<0.2$, data are messy then gradually reach a constant with increasing of *Z/H*. However, at about *Z/H*=0.7 the turbulence intensity increase in diverging sections and it probably due to the presence of hydraulic jump. The theoretical curve was proposed by Nezu and Nakagawa (1993) based on hot-film data of smooth open-channel flows. The deviation of T_u/u_*, T_v/u_* and T_w/u_* from theoretical curve indicate that channel width variation can adjust the distribution of turbulence intensity in another way. To further analyse the effects of channel width variation on flow characteristics, a numerical model will introduced to simulate flows with various flow rates in the same boundary configuration.

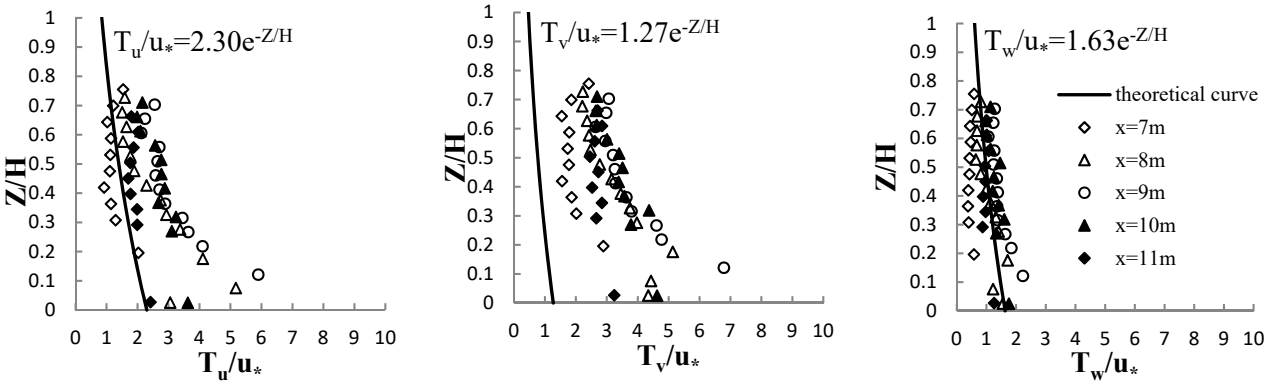

Figure 7. Turbulence intensities profiles in mid-wide line of typical cross-sections (Q=0.1m^3/s, T_u: T in *x*-direction, T_v: T in *y*-direction, T_w: T in *z*-direction, T: Turbulence intensities)

4. Numerical Model

4.1 Governing equation

The conservation form of continuity equation and momentum equation for two-dimensional water flows represents,

$$\frac{\partial C_\xi C_\eta H\Phi}{\partial t}+\frac{\partial(C_\eta Hu\Phi)}{\partial \xi}+\frac{\partial(C_\xi Hv\Phi)}{\partial \eta}=\frac{\partial}{\partial \xi}\left(H\Gamma\frac{C_\eta}{C_\xi}\frac{\partial\Phi}{\partial\xi}\right)+\frac{\partial}{\partial \eta}\left(H\Gamma\frac{C_\xi}{C_\eta}\frac{\partial\Phi}{\partial\eta}\right)+S \tag{1}$$

Where, C_ξ、C_η is Lame coefficient; H is water depth; t is simulated time; u、v is longitudinal velocity function and transverse velocity function, respectively; and $\Phi$is flux, Γ is diffusion coefficient, S is source term. The source term can be linearized as $S=S_c+\Phi_o S_o$. In this equation, S_c represents the constant part of source term; Φ_o is the value in grid central and S_o is a coefficient. Eq.(1) is solved by using finite volume method(FVM) based on orthonormal curvilinear grid, one can get the basic discrete equation,

$$a_o\Phi_o=a_E\Phi_E+a_W\Phi_W+a_N\Phi_N+a_S\Phi_S+b \tag{2}$$

Where, a is a coefficient and b is a constant. Subscript (O、E、W、N、S)represent the position of calculating point in a grid. Adopting the power-law scheme proposed by Patankar, then we have,

$$A(|P|)=MAX(0,\ (1-0.1|P|)^5) \tag{3}$$

Where, $P=\rho uL/\Gamma$ (ρ:fluid density; u:velocity; and L:length) is a ratio of convection intensity and diffusion intensity what we call the Peclet number.

4.2Computational Grid and Boundary Conditions

The orthogonal body-fitted curvilinear coordinate is generated by solving the Possion equation. To avoid generating wavy velocity field, momentum equation is discretized in staggered mesh system, that is locate the velocity calculating point at interface of control mass, missing half grid of depth calculating point. The transition of the irregular physical domain and the regular computational domain satisfy the Possion equation:

$$\xi_{xx} + \xi_{yy} = P(\xi, \eta) \tag{4}$$

$$\eta_{xx} + \eta_{yy} = Q(\xi, \eta) \tag{5}$$

Where, *(x,y)* denote Cartesian coordinates, *(ξ,η)* denote Body-fitted coordinate, *P* and *Q* are regulatory factor to control the density of grid, which can adjust grid's position to fit the boundary in a better way, and keep orthogonal. We will select the expression of *P* and *Q* proposed by J F Thompson. Above methodology is used in the experimental flume, which is shown in Figure 3.

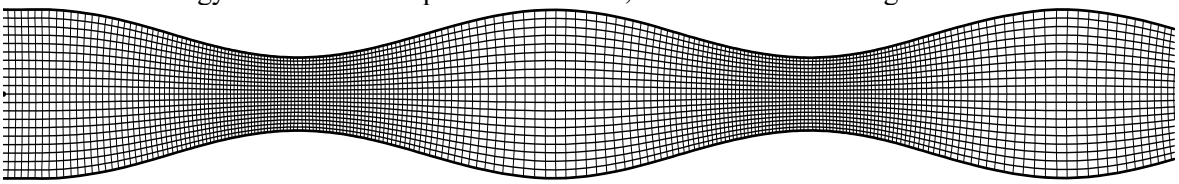

Figure 8. Plan view of grid for experimental flume

To solve the equations presented before, initial and boundary conditions are required at each computational boundary. At the inlet boundary, rate of flow was set. A stage hydrograph was adopted as the outlet boundary condition. At the channel sidewalls, the no-slip boundary condition was specified. Initially, the velocity field was set to zero. The initial water level in computation domain was interpolated accroding to the water level at inlet and outlet section. Meanwhile, traverse gradient was not included in caculating process.

4.3Model Verification

Data obtained from caculation and experimental measurement were compared to verify the numerical model when flow rate was 0.112m^3/s. By comparing velocity and depth in central plan and velocity field in typical sections (see Figure 9 and Figure 10), it is evident that the computed results agree well with experimental data in the flume. The flume is symmetrical about x axis, so data in half-width of every crosss-section are measured. This is why there are zones where experimental data absent. The location deviation of computed results from experimental data in velocity field can mainly be attributed to the difference between computational grid and arrangment of measured profiles. From Figure 10, it is a proof that channel width variation can affect vector which diverge in diverging sections and converge in converging sections.

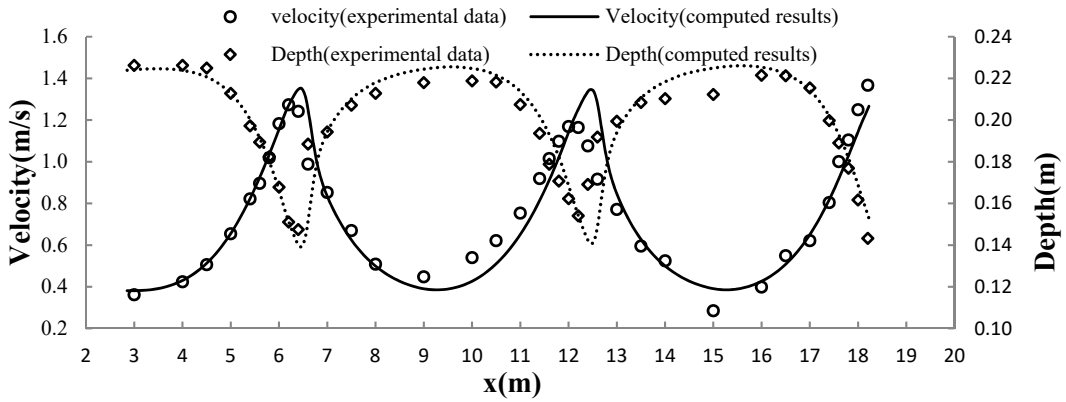

Figure 9. Velocity and depth in central vertical plan

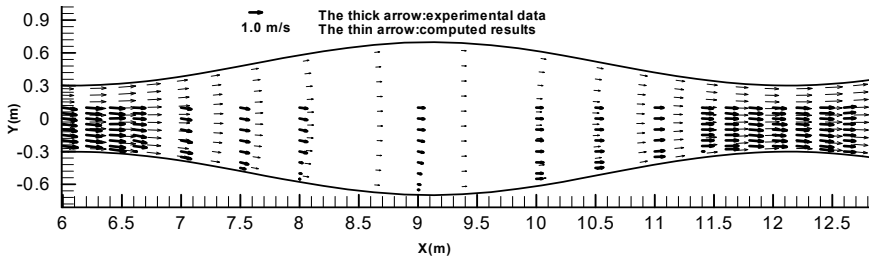

Figure 10. Velocity field in typical sections

4.4 Model Applications

In this part, the numerical model is used to simulate flow structures with different flow rates (Q=0.05m^3/s, 0.2m^3/s, 0.3m^3/s, 0.4m^3/s, 0.5m^3/s, 0.6m^3/s) in the experimental flume. The Froude number (Fr) is an important factor to describe flow pattern, when Fr>1, the flow is supercritical flow while becomes subcritical flow when Fr<1. So Figure 11 is another proof that channel width variation will change flow pattern. On the other side, the range of flow region in supercritical reducing with increasing of flow rates and finally change from supercritical to subcritical flow in diverging sections (it can be clearly seen in the two enlarged pictures in Figure 11). However, the Froude number barely change in different flow rate of converging sections. Meanwhile, the diverging sections downstream can also affect the flow structures in upstream. When Q=0.5m^3/s, different flow patterns occur in the same position of diverging sections between upstream and downstream, such as Fr<1 at x=6.3m but Fr>1 at x=12.3m. It can be ascribed to backwater produced by the narrowest section downstream.

As all known, hydraulic jump is a transition from supercritical to subcritical flow. There are three hydraulic jump patterns which are submerged jump, critical jump and remote jump. Submergence happens when the sequent depth (h_m) exceeds conjugate depth in contracted section and remote jump happens when the sequent depths is lower than the conjugate depth, otherwise critical jump occurs when the sequent depth equal to the conjugate depth. To analysis jump patterns in converging regions, formula (6) was introduced to calculate the conjugate depth.

$$h_0' = 2h_0\sqrt{\frac{1+\xi+4\beta Fr_0^2}{3(1+\xi)}}\cos\frac{\psi}{3} \tag{6}$$

Ψcan be obtained as:

$$\cos\psi = -\frac{10.4\beta(1+\xi)^{0.5}Fr_0^2}{\xi(1+\xi+4\beta Fr_0^2)^{1.5}} \tag{7}$$

Where, h_0' is conjugate depth in contracted section. Fr_0 is Froude number in contracted section. β is momentum correction factor, when diffusion angle θ<25°, β=1.03. $\xi=B_m/B_0$, B_m, B_0 are width in sequent section and contracted section, respectively. The results are shown in Figure 12, which hydraulic jumps happen in the flume are almost submerged jumps.

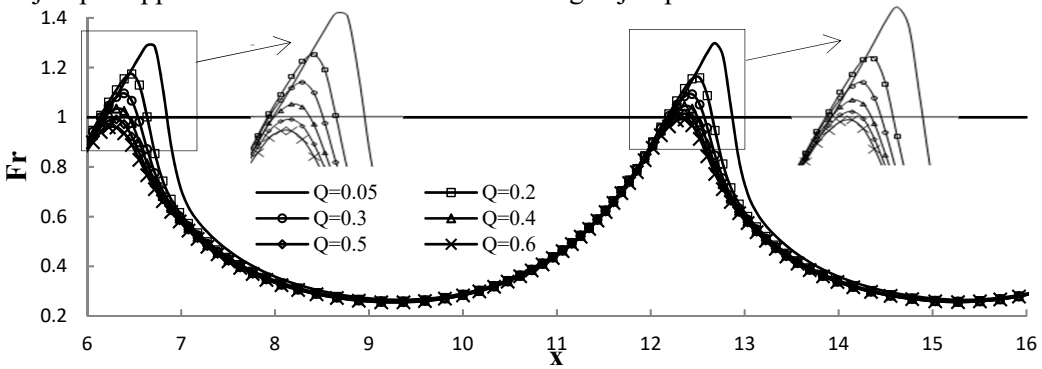

Figure 11. Froude number in difference flow rates

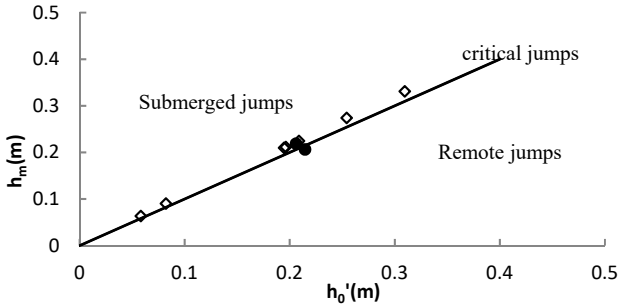

Figure 12. Comparison between sequent depth and conjugate depth

5. Conclusions

This paper presents the results of a laboratory and numerical study on the flow characteristics in a flume with width changing. It is found that the longitudinal water depth and velocity change along with the transition width of flume. Depth increase and velocity decrease in diverging region, while go the opposite way in converging region. Whether in diverging sections or converging sections, velocity along the vertical in mid-wide line of typical cross-section decreases with increasing of channel width and water depth. Besides, river width changes also affect distribution of turbulence intensities. The turbulence intensities increase with increasing of channel width, and the turbulence intensity distribution in x-direction are similar to that in y-direction, which are both stronger than that in z-direction. Furthermore, the Froude number decreases with increasing width which values are greater than one in region near the narrowest section where supercritical flow occurs.

The comparison between the experimental results and computed results show that the numerical model can simulate flow characteristics in the width changing river appropriately. To further analysis the effects of river width changes on flow characteristics, the numerical model was used to simulate the gradual channel transition flow in various flow rates. When the flow rate increases, the range of flow region in supercritical flow reduces and flow pattern changes from supercritical to subcritical flow at last in diverging sections. The hydraulic jumps which occur in diverging region are almost submerged jumps and the degree of submergence increases with increasing of flow rate.

Acknowledgments

The work was partially supported by the projects of National Key R&D Program of China (Grant No. 2017YFC0405306).

References

[1] Afzalimehr H and Anctil F O 2000 Accelerating shear velocity in gravel-bed channels *J. Hydrolog. Sci.* **45** (1): 113-124.
[2] Armellini A, Casarsal L and Giannattasio P 2009 Separated flow structures around a cylindrical obstacle in a narrow channel *Experimental Thermal and Fluid Science* **33**(4): 604-19.
[3] Blanckaert K and Vriend de H J 2005 Turbulence characteristics in sharp open-channel bends. *Physics of Fluids* **17** (5): 055102.
[4] Barbhuiya A K and Talukdar S 2010 Scour and three dimensional turbulent flow fields measured by ADV at a 90°horizontal forced bend in a rectangular channel *Flow Measurement and Instrumentation* **21**: 312-21.
[5] Lucy C, Quine T A and Nicholas A 2010 An experimental investigation of autogenic behavior during alluvial fan evolution *Geomorphology* **115**(3/4): 278-85.
[6] Nezu I. and Nakagawa H. 1993 Turbulence in open-channel flows (Rotterdam: Balkema)
[7] Nguyen T H, Rob B, Marcel J F, Stive and Henk J V 2007 Deceleration open-channel flow in gradual expansion *Asian and Pacific Coasts* (Nanjing China.)
[8] Paiement-Paradis G, Marquis G and Roy A 2011 Effects of turbulence on the transport of individual particles as bedload in a gravel-bed river *Earth surface processes and landforms*

36(1): 107-16.
[9] Papanicolaou A N and Hilldale R 2002 Turbulence characteristics in gradual channel transition. *J. Eng. Mech.* **128**: 949-60.
[10] Singha A and Balachandar R 2011 Structure of wake of a sharp-edged bluff body in a shallow channel flow, *Journal of Fluids and Structures* **27**(2): 233-49.
[11] Thomas M and Chaudhry M H 1995 Depth-averaged open-channel flow model *Journal of Hydraulic Engineering* **121**(6):453-465.
[12] Wang X Y, Yang Q Y, Lu W Z,Wang X K 2011 Experimental study of near-wall turbulent characteristics in an open-channel with gravel bed using an acoustic Doppler velocimeter. *Exp. Fluids* **52**: 85-94.
[13] Weber L J, Eric D S, and Nicola M 2001 Experiments on flow ata 90° open-channel junction. *J. Hydraul. Eng.* **127**(5):340–50.
[14] Yan X F, Yi Z J, Liu T H, Liu X N and Wang X K 2011 Flow Structure and Characteristics of Local Head Loss in Transition Channel *Journal of Yangtze River Scientific Research Institute* **28**(9):1-5.